Compensation of Presbyopia With the Light Sword Lens

Alejandro Mira-Agudelo,[1] Walter Torres-Sepúlveda,[1] John F. Barrera,[1] Rodrigo Henao,[1] Narcyz Blocki,[2] Krzysztof Petelczyc,[3] and Andrzej Kolodziejczyk[3]

[1]Grupo de Óptica y Fotónica, Instituto de Física, Facultad de Ciencias Exactas y Naturales, Universidad de Antioquia UdeA, Medellín, Colombia
[2]Maksymilian Pluta Institute of Applied Optics, Warsaw, Poland
[3]Faculty of Physics, Warsaw University of Technology, Warsaw, Poland

Correspondence: Alejandro Mira-Agudelo, Grupo de Óptica y Fotónica, Instituto de Física, Facultad de Ciencias Exactas y Naturales, Universidad de Antioquia UdeA, Calle 70 No. 52-21, Medellín, Colombia; alejandro.mira@udea.edu.co.

Submitted: March 2, 2016
Accepted: October 10, 2016

Citation: Mira-Agudelo A, Torres-Sepúlveda W, Barrera JF, et al. Compensation of presbyopia with the light sword lens. *Invest Ophthalmol Vis Sci*. 2016;57:6870–6877. DOI: 10.1167/iovs.16-19409

Purpose. We present the first physiological evaluation of the use of the light sword lens (LSL) for presbyopia compensation. The LSL is an axially asymmetric optical element designed for imaging with extended depth of focus.

Methods. A monocular visual simulator setup is implemented to measure visual acuity (VA). Physiological presbyopia is "mimicked" in human subjects by paralysis of the ciliary muscle, using topical application of a muscarinic antagonist. The effect of a contact lens-configured LSL on the mimicked presbyopia visual system is evaluated by measuring VA as a function of target vergence. The ability of the LSL to compensate presbyopia for 2 photopic luminance values was also analyzed.

Results. The average VA values for 11 subjects suggest that the LSL can compensate for presbyopia across a wide range of target vergences for which the LSL was designed (−3 to 0 D). However, the proposed corrector element causes a loss of distance VA. The mean logMAR VA in that target vergence range was 0.07. The VA curves also show that luminance does not affect the expected behavior of the LSL-corrected presbyopic eye.

Conclusions. These results indicate that the LSL has significant potential as a visual aid for presbyopia.

Keywords: aging changes, ophthalmic optics, presbyopia, vision acuity, visual optics

Presbyopia is the decrease in accommodative amplitude of the human visual system that occurs with aging of the eye.[1] Although presbyopia is a progressive vision disorder that affects everyone after a certain age,[2] there is no effective way to prevent it. Therefore, over the last 2 decades, important optical investigations have been undertaken to find ways to compensate for this visual condition.

Over time, different optical methods to correct presbyopia and restore the ability to recognize both distant and near objects have been proposed.[3–6] Some proposals include reading glasses, monovision, residual myopia, multifocal lenses used in glasses, contact lenses, and intraocular lenses. Multifocal intraocular lenses usually are bifocal or trifocal.[7,8] Recent proposals include modifying the topography of the cornea with refractive surgery[4] or inserting a small-aperture (pinhole) implant to artificially reduce the size of the pupil and generate a wider depth of focus.[9]

Other possible ways to correct presbyopia include varifocal elements based on the Alvarez lenses[10] or programmable lenses based on spatial light modulators,[11,12] which are classified as accommodative lenses. In addition, adjustable lenses that attempt to mimic how the eye lens functions have been designed,[13,14] and changing the optical power by axial displacement of a lens of a fixed focus has also been implanted and tested.[15,16]

Despite multiple proposals and scientific advances, there is still no entirely satisfactory way to correct presbyopia. For some proposals, the applied correction improves vision for only some fixed distances instead of for a continuous range of distances. With other proposals, optimal vision cannot be achieved under low-luminosity conditions, they are expensive and technologically difficult to fabricate, they do not work in real time, or they present clinical and physiological restrictions.

In the last 10 years, optical elements with extended depth of focus that compensate for presbyopia have appeared. These elements allow the subject to recognize objects at different distances. These optical elements include axicons with an axial symmetry profile[17] and some structures with an asymmetrical profile such as the cubic phase mask,[18] the peacock eye optical element,[19] and the light sword lens (LSL).[20]

Previous studies have proposed use of the LSL to correct presbyopia[20–24] because it was designed to image objects at a wide range of distances. Performance of the LSL as a corrector element was evaluated recently by means of objective experiments using a simplified model of a presbyopic eye.[24] The results demonstrated that the LSL in a contact lens configuration significantly improves the visual acuity (VA) of a monofocal optical system within a wide range of defocus. Results from the objective experiments and numerical simulations[22,23] showed that the performance of the LSL is superior to other available solutions. However, psychophysical tests are necessary to study the actual behavior of the LSL. Such subjective tests allow evaluation of the practicality of the LSL for presbyopia compensation and the improvement of the principal visual parameters that quantify this correction.

Motivated by this necessity, we present our psychophysical evaluation of the performance of the LSL in presbyopia compensation. We measured the VA of several subjects by

FIGURE 1. (*Left*) Focusing geometry of the LSL. (*Right*) Shape of the LSL.

using a monocular visual simulator (MVS). In addition, we analyzed the effect of changing the luminance of the system. The MVS enables noninvasive subjective experiments to study the visual performance of elements like lenses, plates, or phase profiles.[25]

This work was the first subjective evaluation of the LSL using real human eyes (Torres W, et al. *IOVS* 2015;56:ARVO E-Abstract 2981), and the results agreed with those of previous objective experiments.

The LSL is proposed as a way to solve the decrease in the accommodation range of human vision. This optical element focuses an incident plane wave or spherical wave around an axial line segment. Following geometrical optics, the LSL focuses a plane wave from a distance, f_a, up to a distance f_b.[20] Each angular sector of the LSL focuses light into a perpendicularly oriented small strip (Fig. 1, left panel).[23]

The optical properties of the LSL and its imaging with extended depth of field have been widely studied numerically and experimentally.[20–24,26,27] These investigations confirmed that the images formed by the LSL have acceptable resolution and contrast. Therefore, lenses with angular modulation of optical power such as the LSL can be useful for imaging with extended depth of field. Therefore, angularly modulated structures can be used successfully in machine vision and ophthalmic applications. The first experimental results showed that use of a refractive LSL does not exhibit significant chromatic aberrations compared with the corresponding diffractive version. This way, the refractive LSL can be used for imaging with extended depth of field in polychromatic light.[21] Moreover, computational results demonstrated the uniformity of Strehl's ratio of the LSL, which is almost constant along the entire length of the focal segment.[26] The ability of the LSL to correct presbyopia was studied in a model of the presbyopic human eye illuminated by white light.[22] The results showed that the LSL enables defocus compensation in the range of 0 to 4 D. These properties make the LSL valuable for ophthalmic applications and for presbyopia correction in particular. A recent study[24] analyzed the simulated acuity of functional vision obtained using a refractive version of the LSL. The experimental setup included an artificial eye based on Gullstrand-Emsley parametrization and an LSL that acted as a contact lens. From experimental results, one can conclude that the LSL is suitable for ophthalmic applications, especially for correcting presbyopia.

The LSL in refractive form (Fig. 1, right panel) presents a nonsymmetrical profile described by the shape function[24]:

$$\Delta l(r,\theta) = l_{\max} - \frac{\Delta D \theta r^2}{4\pi(n-1)} \qquad (1)$$

where $l_{\max}$ is the maximal thickness of the element, n is the refractive index of the LSL, ΔD is the maximal addition of optical power, and θ and r are the angular and radial coordinates, respectively. According to Equation 1, the differences in thickness are proportional to the angular coordinates (Fig. 1, right panel).

METHODS

Experimental Setup

The LSL used in our experiments was the same as that validated by Kakarenko et al.,[24] with $\Delta D = 3$ D. The element was fabricated in poly(methyl methacrylate) (PMMA) through molding injection by using a micromachining technique.

The schematic diagram of the MVS setup used to measure VA is shown in Figure 2. The MVS consists of three parts: a Hartmann-Shack sensor (HSS), a stimulus pathway, and a Badal lens system (BLS). In the first part, the pupil is optically conjugated to the HSS[28] by means of a telescopic system formed by the pairs of achromatic lenses L2 to L5; the HSS measures the ocular aberrations of the subjects by using a diode laser, which emits invisible near-infrared light of wavelength $\lambda = 980$ nm to illuminate the eye after reflection on a pellicle beam splitter. The second part includes a cathode ray tube computer monitor with a resolution of 192 pixels per degree. The monitor displays the visual stimulus in white light for the vision tests. The third part contains a BLS that corrects the refractive error of the eye and also induces the desired target vergence. These processes are done by changing the vergence of light that passes through the BLS, but the angular size of the objects is not modified, so it is not necessary to move the monitor for every test. The BLS has a power range from –4 to 4 D to generate positive (convergent wavefront) and negative (divergent wavefront) vergences. The BLS contains a pair of achromatic lenses (L2 and L3) and 4 mirrors (M2 to M5). Mirrors M3 and M4 make up the translation stage that generates the desired vergence when it is displaced. The distance between L2 and the pupil of the subject is equal to the focal length of L2. The three conjugated planes of the pupil in the MVS correspond to the positions of the LSL, the HSS, and the artificial pupil. The conjugated plane in which the LSL is placed in a contact lens configuration is obtained by means of lenses L2 and L3 in the BLS. A hot mirror allows positioning of the HSS and the artificial pupil in the remaining conjugated planes.

Lenses L2 and L3 have a 15-cm focal length, producing a magnification equal to unity. Lenses L4 and L5 have 20-cm and 10-cm focal lengths, respectively, and the afocal system formed by these lenses has a 2.0× magnification (seen from computer monitor to the subject's eye). In this case, the artificial pupil size is 2.05 mm, but the pupil size at the LSL and subject's pupil planes is 4.1 mm due to such magnification. This pupil size corresponds to the average for a presbyopic subject (55 years of age) in photopic illumination.[29]

The artificial pupil has two functions: (1) it controls the amount of light processed by the system, and (2) it ensures proper illumination of the LSL. The remaining section of the monocular visual stimulator contains the He-Ne laser, the spatial filter, lens L1, and mirror M1. This section is used to align and calibrate the setup.

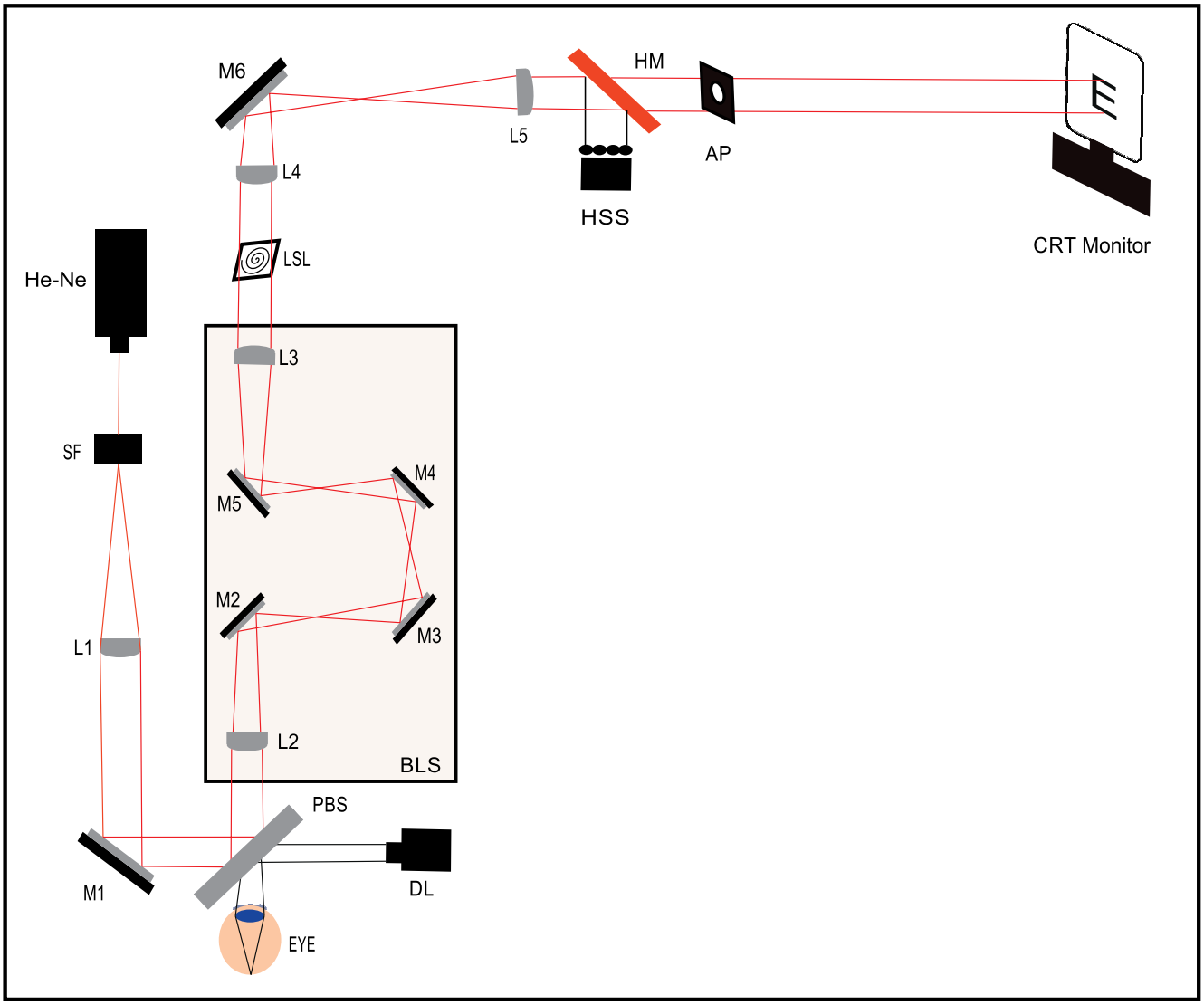

Figure 2. Schematic of the monocular visual simulator (MVS) setup. AP, artificial pupil; BLS, Badal lens system; CRT monitor, cathode ray tube computer monitor; DL, diode laser; He-Ne, helium-neon laser; HM, hot mirror; HSS, Hartmann-Shack sensor; L, achromatic lens; LSL, light sword lens; M, mirrors; PBS, pellicle beam splitter; SF, spatial filter system.

Subjects

Eleven subjects between 18 and 35 years of age (mean = 25 years) participated in the study. Presbyopia was mimicked in each subject by paralysis of the ciliary muscle, using topical application of a muscarinic antagonist. This causes temporary cycloplegia and mydriases; the cycloplegia is used to mimic the small amplitude of accommodation of presbyopic human subjects. The differences in spherical aberration between young and old subjects was not considered. The study was performed in the dominant eye (sighting dominance) of each subject. The subjective refractions of the participants were measured using the BLS after inducing temporary cycloplegia and mydriasis. Those refractions were in the range of –1.6 to +0.7 D, with an average value of –0.4 ± 0.7 D, and the best-corrected distance VA (BCDVA) was in the range of –0.18 to 0.01 D (logMAR scale) with –0.07 ± 0.06 D on average. The astigmatism of the subjects was within the range –0.6 to 0.0 D, with a mean of –0.3 D and a standard deviation of ± 0.2 D. The average pupil size of the subjects was 7.4 ± 0.5 mm (after inducing temporary mydriasis), within the range of 6.8 to 8.0 mm (these pupil sizes were measured using the HSS); these values ensured that the 4.1-mm artificial pupil size was smaller than the dilated pupil size in all cases. Thus, this ensured that the measurements were taken using a pupil size that corresponded with the average pupil size of a 55-year-old presbyopic subject.[29] Informed consent was obtained from the subjects after explaining the nature and possible consequences of the study.

Measurement Protocol

The measurement protocols followed the tenets of the Declaration of Helsinki,[30] and the study was approved by the Bioethics Committee of the University Research Center (Sede de Investigación Universitaria) from the University of Antioquia, Medellín, Colombia. To mimic presbyopia, cycloplegia was induced by applying 2 drops of 1% tropicamide ophthalmic solution at the beginning of the experimental session and 1 extra drop after each hour of measurements; this is a standard procedure in this kind of study.[31–33] We found the BCDVA using the BLS after induction of cycloplegia. The

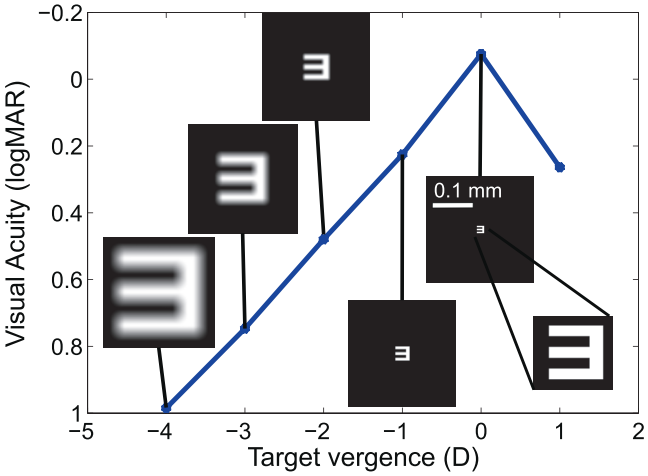

FIGURE 3. Experimental VA (on a logMAR scale) as a function of target vergence for a naked eye with mimicked presbyopia. Target vergence values are in diopters and increase with the distance of the object. The images are simulations meant to show the effect of pure defocus in a fixed-focus imaging system. The denoted scale in the inlayed images refers to the retina plane.

effectiveness of tropicamide was verified by obtaining the typical VA through-focus curve for a cycloplegic eye for all subjects (see Fig. 6a) and finding little variation in the subjective measurement of the refraction. A bite bar was used during all tests to stabilize and align the subject. In addition, the alignment of the subject was controlled using the HSS, which was initially aligned with the LSL and the artificial pupil planes, and the diode laser, which had a maximum power of 30 μW. The reference point for the alignment of the eye was the center of the entrance pupil of the subject's eye. Refraction was corrected with the BLS after proper alignment to obtain a target vergence of 0 D. With the BLS properly positioned, the HSS was used to obtain a video to measure the ocular aberrations of the subject and thus determine the astigmatism. Then the BLS generated target vergence from −4 to +1 D in steps of 1 D (i.e., −4, −3, −2, −1, 0, and +1 D). A forced-choice test using FrACT version 3.8.0e software (Michael Bach, Sektion Funktionelle Sehforschung, Universitäts-Augenklinik, Freiburg, Germany) was performed to find the VA of the subject in each target vergence. The test was based on the Snellen-E optotype recognition test in which four different orientations and the best parameter estimation by sequential testing (PEST) adaptive method were used to determine the threshold size of optotype recognized after 48 trials.[34] The complete set of measurements was repeated to estimate the experimental error. Visual acuity of the naked eye, that is, without correction, was measured under high luminance condition of HL1, which is equal to 100 cd/m^2, and then with the LSL, with a power range of 0 to +3 D, located in the pupil conjugated plane (Fig. 2). Finally, the measurements were repeated with another high luminance value of HL2 equals to 30 cd/m^2, where neutral density filters reduced the luminance to 30% of the initial level, preserving the photopic condition. The measurements took 2 h with a 10-min break after the first hour.

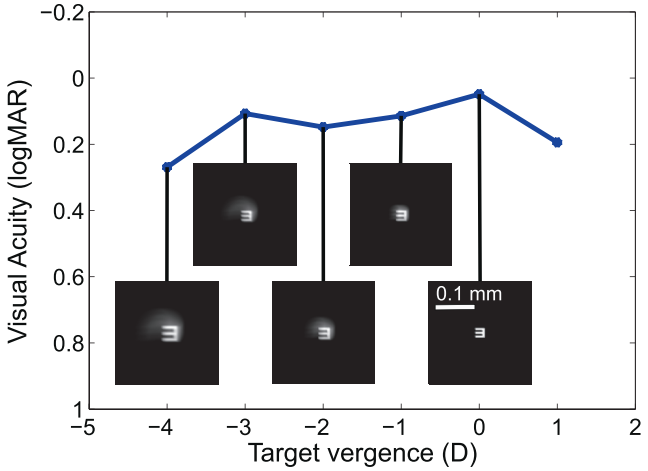

FIGURE 4. Experimental VA (on a logMAR scale) as a function of target vergence for an eye with mimicked presbyopia corrected by the LSL. Target vergence values are in diopters and increase with the distance of the object. The images are simulations meant to show the effect of pure defocus in a fixed-focus imaging system with the LSL. The denoted scale in the inlayed images refers to the retina plane.

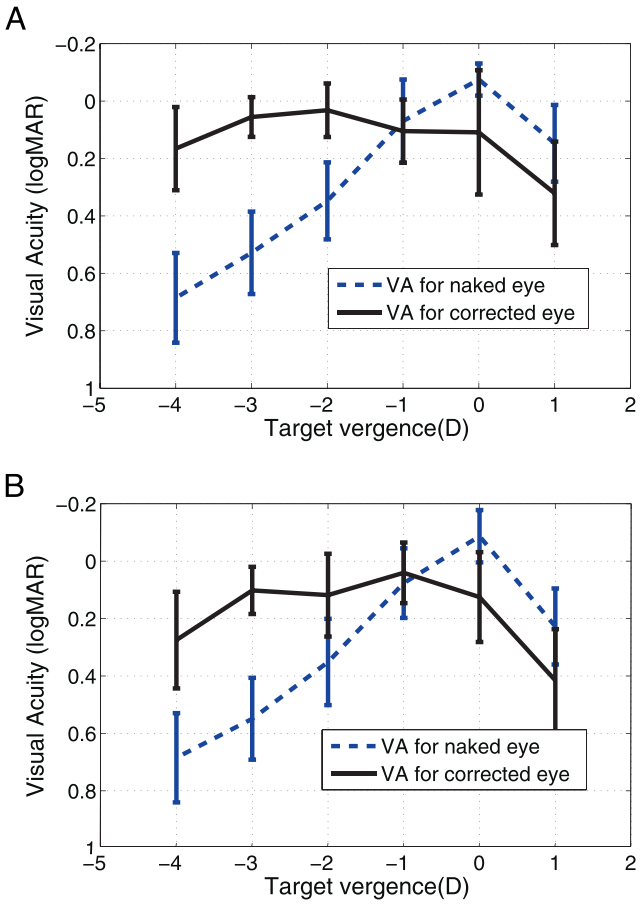

FIGURE 5. Average VA (on a logMAR scale) as a function of target vergence for 11 eyes with mimicked presbyopia under two high-luminance conditions (**A**) HL1 equals to 100 cd/m^2 and (**B**) HL2 equals to 30 cd/m^2. *Dashed blue curves* show the average VA for the naked eye (without LSL), and *continuous black curves* show the average VA for the LSL-corrected eye. Target vergence values are in diopters and increase with the distance of the object. *Error bars:* ±1.0 SD.

RESULTS

Figures 3 and 4 show the results of the VA tests as a function of defocus for one subject. The figures also include images obtained via simulation that are meant to show the expected effect of pure defocus in a fixed-focus imaging system (as a

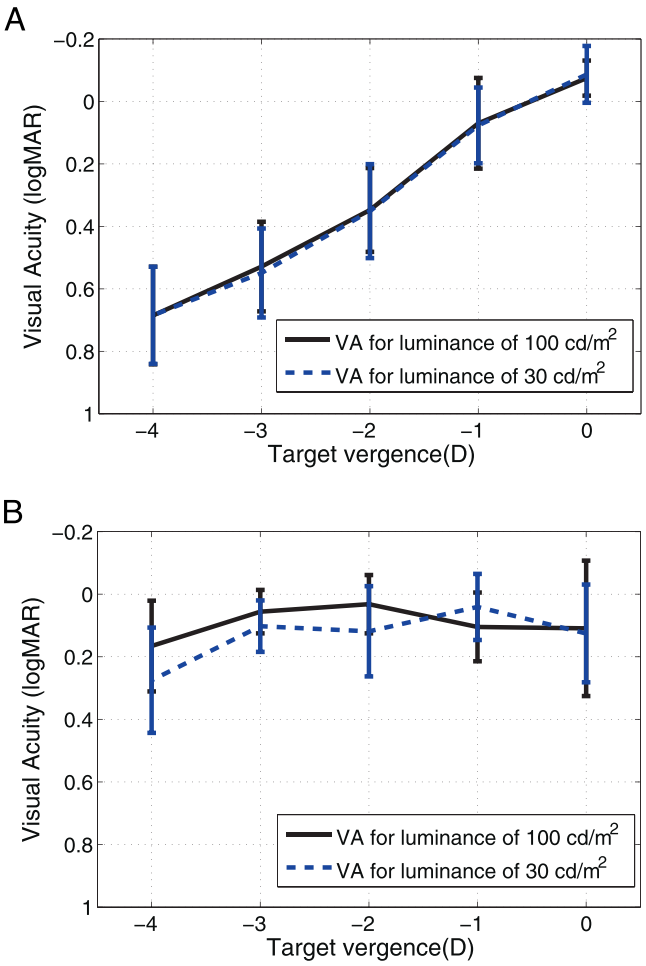

FIGURE 6. Average VA (on a logMAR scale) as a function of target vergence for 11 eyes with mimicked presbyopia for both high luminance conditions (**A**) without correction and (**B**) with the LSL. *Dashed blue curves* show the average VA for luminance HL2, and *continuous black curves* show the average VA for luminance HL1. Target vergence values are in diopters and increase with the distance of the object. *Error bars*: ±1.0 SD.

simplified representation of a naked presbyopic eye) and the expected effect in that ideal system with the LSL as the corrective element. The convolution method using spatially incoherent light was used to obtain the images. In this method, the generalized pupil function was the result of the LSL transmittance multiplied by a phase factor given by the wave aberration function including only the defocus term. Then the expected image intensity was the convolution of the squared modulus of the Fourier transform of the generalized pupil function (the point spread function in the incoherent case) with the ideal image intensity.[35] The convolution process was performed for several defocus values. The implemented simulation to obtain the images used a 12,000 × 12,000-point matrix with a 1 μm sampling interval that covered a square area and was 12 mm wide. In Figure 3, the best VA for the naked eye was for far vision (0 D), whereas it quickly got worse at other target vergence stages, as was expected from the simulated images. On the other hand, in Figure 4, VA for the eye corrected with the LSL remained acceptable in the target vergence range of −3 to 0 D. Note that the LSL used in this experiment was designed for an optical power range of 0 to +3 D.

Comparison of Figures 3 and 4 shows the effect of the LSL on vision. The best VA with the naked eye occurs at 0 D, whereas VA is significantly better in the range −4 to −1 D after correction with the LSL (Fig. 4).

In order to evaluate the performance of the LSL under two photopic illumination conditions, we averaged the results obtained for the luminance values of HL1, which equals 100 cd/m^2, and HL2, which equals 30 cd/m^2 for the 11 subjects, following the experimental protocol; the results are presented in Figure 5.

Figure 5a presents the average VA under the high-luminance condition HL1 as a function of target vergence for the naked presbyopic eye and the presbyopic eye corrected with the LSL. For the naked eye, the plot is similar to that in Figure 3, with the best VA at 0 D and a tendency for worsening VA until logMAR VA is 0.7 (18% of the maximal VA on a decimal scale) at a target vergence of −4 D. For the LSL-corrected presbyopic eye, the average VA remained almost constant in the target vergence range of −3 to 0 D, similar to that shown in Figure 4. The mean logMAR VA in the target vergence range of −3 to 0 D was 0.07 (75% of the maximal VA on a decimal scale), whereas the logMAR VA values were >0.17 (60% of the maximal VA on a decimal scale) for the other target vergence stages.

Figure 5b shows the VA results for the high-luminance HL2. The VA for the naked presbyopic eye in luminance HL2 trends the same way as that in luminance HL1. For the LSL-corrected eye, VA in the target vergence range of the LSL of −3 to 0 D was almost constant, with a mean logMAR VA of 0.09 (68% of the maximal VA on a decimal scale), whereas the logMAR VA values were >0.25 (48% of the maximal VA on a decimal scale) for the other target vergence stages.

The curves of the averaged VA of the 11 mimicked presbyopic subjects with and without LSL compensation for both of the high-luminance conditions (Figs. 5a, 5b) have the same shapes as those in Figures 3 and 4. However, the averaged results for the LSL were significantly better than those in the naked eye only in the range −4 to −2 D. At −1 D, the performance was identical in both of the cases, whereas the naked eye performed better at 0 and +1 D.

Figure 6 presents the same plots as those in Figure 5 but directly compares the VA at both luminance values for the naked presbyopic eye (Figure 6a) and the LSL-compensated eye (Fig. 6b). These figures show the target vergence only in the range −4 to 0 D, considering the +1 D target vergence as a control value (+1 D is a virtual object with no associated distance in a real scene). The trend for the naked eye was similar for both of the photopic luminance conditions. The trend for the compensated eye in HL1 and HL2 luminance values was similarly constant, although the average VA values for HL1 were better than those for HL2, except for a target vergence of −1 D. Figure 6a shows the expected behavior of the naked presbyopic eye, with a steady worsening of VA as the target vergence increased. Each error bar in Figure 6 was calculated using the standard deviation in VA for the 11 subjects. The VA used depended on the quality of vision of the individual, which explains the dispersion seen in the error bars.

DISCUSSION

We performed a three-way analysis of variance (ANOVA) test of the results.[32,36] This global analysis showed that over the VA there was a main effect due to the target vergence (range of −4 to 0 D) and the correction condition (naked eye, LSL-corrected eye), giving a P value of 0.0001 for both factors (Table). A P value of 0.3958 for the luminance level factor showed that the

Table. Three-Way ANOVA of Results in Figure 6*

Factor	*P* Value
Target vergence	0.0001
Correction condition	0.0001
Luminance level	0.3958
Target vergence * correction condition	0.0002
Target vergence * luminance level	0.4081
Correction condition * luminance level	0.1206

* This test compares the mean VA values as a function of the target vergence state (range, –4 to 0D), the correction condition (naked eye, LSL-corrected eye), the luminance value (HL1 = 100 cd/m^2; HL2 = 30 cd/m^2), and the interaction among these three factors.

VA values were not statistically different for a luminance of HL1 equal to 100 cd/m^2 and an HL2 equal to 30 cd/m^2.

Likewise, *P* values of 0.4081 and 0.1206 for the interaction terms "Target vergence * Luminance level" and "Correction Condition * Luminance level," respectively, showed no statistically significant interaction effects for either term, which are noted in Figure 6.

Therefore, a change in luminance does not affect the general performance of VA with or without the correction, where the size of the artificial pupil remains constant. This is an important feature of the LSL in addition to its ability to correct presbyopia.

On the other hand, the *P* value of 0.0002 for the interaction term "Target vergence * Correction Condition" strongly indicates that the effect of the target vergence over the VA depends on the correction condition.

In order to analyze this interaction, a post-hoc study was conducted to find which combination levels from these two factors were related with the VA change. More specifically, a pairwise analysis was applied to the data by means of a Tukey test to determine which of those combinations led to statistically significant variations of the VA.

For the naked eye condition, the pairwise analysis combined all target vergence states evaluated in the ANOVA test, and it gave *P* values in the range of 0.0001 to 0.0496.

These results show that the VA values are statistically different (not constant) in the target vergence states in the range of –4 to 0 D, with an uncertainty below 5%. This expected nonconstant behavior of the VA for the target vergence in the naked presbyopic eye can be seen in Figure 6a and in the first 5 cases of Figure 7, which summarize all mean VA values involved in the pairwise analysis.

On the other hand, a relatively constant VA in the range of –4 to 0 D was obtained for the LSL-corrected presbyopic eye (Fig. 6b). For that case, the pairwise analysis over the VA values for all target vergence levels in the mentioned range shows that it is not possible to state that the VA values are statistically different (*P* values greater than 0.078 for all target vergence levels with corrected eye condition). If the target vergence levels are delimited to the range that the LSL was design for (i.e., –3 to 0 D), then the *P* values from the pairwise analysis are all equal to 1.0. This implies that the LSL effectively extends the depth of field of the presbyopic eye, yielding an almost constant VA within the designed range of the LSL. This can be seen in the last four cases of Figure 7.

Therefore, a relatively constant VA close to 0.1 (in logMar scale) can be achieved with LSL correction (VA close to 0.2 for –4 D), in contrast to the VA obtained by a presbyopic eye for any target vergence except 0 D (BCDVA). These quantitative results show that the LSL plays a substantial role in the improvement of the VA in mimicked presbyopic subjects for near and intermediate vision. A letter size of 0.1 (in logMar scale) can be seen by a normal naked eye until a defocus of

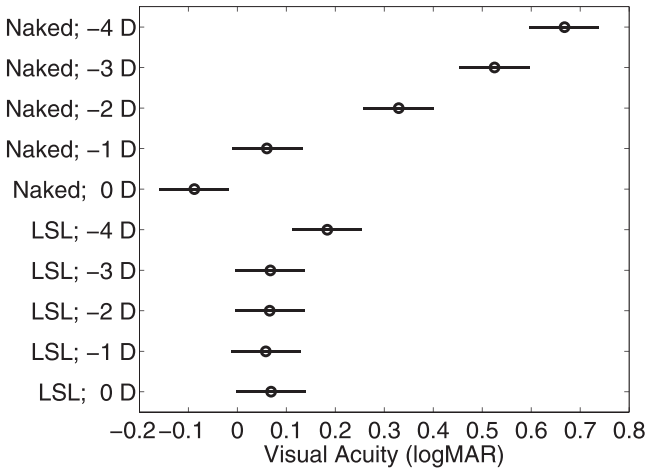

Figure 7. Mean VA values, involved in pairwise analysis, for different levels of target vergence and correction condition factors. "Naked; –4D," "Naked; –3D," "Naked; –2D," "Naked; –1D," and "Naked; 0D" are VA mean values, and their dispersion for the naked eye correction condition in –4D, –3D, –2D, –1D, and 0D target vergence, respectively. "LSL; –4D," "LSL; –3D," "LSL; –2D," "LSL; –1D," and "LSL; 0D" represent VA mean values and their dispersion for the LSL-corrected eye condition in –4D, –3D, –2D, –1D, and 0D target vergence, respectively.

–0.46 D or –0.65 D, which correspond to the limits at which the induced blur just becomes troublesome or objectionable, respectively.[37] Then, from a perceptual viewpoint, a letter size of 0.1 is acceptable.

For distance vision with the LSL there is a loss of 1.7 lines of acuity compared with the BCDVA of the naked presbyopic eye, as demonstrated in Figures 5 and 7. In order to contrast the performance of the LSL with other presbyopia correction approaches, the through-focus VA curves for the naked presbyopic eye (monocular), the LSL-corrected eye (monocular), correction with diffractive trifocal IOL FineVision (binocular) (PhysIOL, Liège, Belgium),[7] traditional monovision[31] (binocular simulator), combined monovision with a small aperture inlay[31] (binocular simulator), correction with diffractive trifocal IOL AT Lisa tri 839MP[8] (binocular) (Carl Zeiss Meditec AG, Oberkochen, Germany), and center-distance Proclear multifocal contact lens[32] (monocular) (Coopervision, Pleasanton, CA, USA) are presented (Fig. 8).

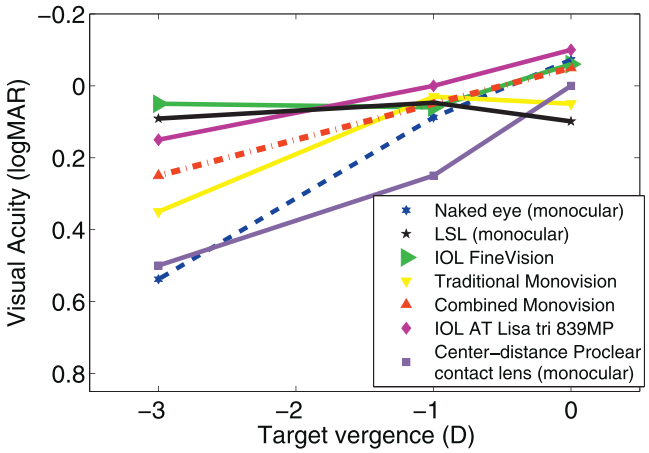

Figure 8. Through-focus VA curves for different presbyopic correction approaches.

The VA values at near and intermediate vision for the LSL presbyopic corrections are similar or better than those of other approaches, whereas for the far vision case, the correction with the LSL does not work very well. The IOL FineVision, IOL AT Lisa tri, and the combined monovision with a small aperture inlay approaches at 0 D, give a gain of two lines of VA compared with LSL correction. Nevertheless, for traditional monovision and center-distance Proclear multifocal contact lens approaches, at the same far view condition, a gain of only one line (or less) of VA is obtained with respect to the LSL correction.

On the other hand, it is important to point out that some of the best results in the mentioned approaches were obtained for binocular VA measurements. As usual, binocular viewing exhibits better VA results than monocular vision. The binocular results by means of the LSL as corrector element would have a better performance.

Although this contribution presents, for the first time, psychophysical evaluation of the visual system with the light sword optical element, additional research is necessary to evaluate the performance of the correction under different circumstances. Future research can include experiments in the mesopic and scotopic ranges, binocular and monovision studies, contrast sensitivity measurements, low-contrast VA testing, and performing experiments using real presbyopic subjects. Also, the profile of the LSL defined by the linear angular function (Equation 1) can be modified to improve the correction in far vision, preserving angular modulation of the optical power. In this direction, a possible solution would be redesigning the LSL profile by assigning some window of the element to correct the far vision, and by molding the angular profile on the remained surface of the element. This approach will require the optimization of the window shape and its area. This possible solution is similar to some previously proposed profiles, such as those reported by Cánovas et al.[38] Another possible way to obtain better results would be to use the LSL in a monovision configuration, so one eye is corrected for far vision and the other one is corrected with the LSL for near and intermediate vision.

Conclusions

In this paper, we presented the first psychophysical experiments that evaluated the ability of the light sword lens to compensate for presbyopia. We used a monocular visual simulator comprising a Hartmann-Shack sensor, a stimulus pathway, and a BLS. The results obtained for the 11 subjects with mimicked presbyopia showed the expected behavior for an uncorrected (naked) presbyopic eye, where the VA peaked at 0 D. In contrast, with the use of the light sword lens as a presbyopia-correcting element, VA became better from −4 to −2 D, identical at −1 D, and worse at 0 D, compared with the naked presbyopic eye. These results obtained using psychophysical evaluation of the visual system show the usefulness of the light sword lens for correcting presbyopia. The VA curves show that the light sword lens can compensate for presbyopia in a wide target vergence range. However, the proposed corrector element presents a loss of VA in distance vision compared with some presbyopic correction approaches. In addition, we studied the behavior of the LSL under two high-luminance conditions. The VA curves clearly showed that the luminance does not affect the expected behavior of the LSL-corrected presbyopic eye. This is an important feature of the LSL in addition to its ability to compensate for presbyopia. Not only are the results presented here from the first experiments performed with human subjects, they also agree well with those of the previous objective analysis of the light sword lens.[24] The results presented here are an important step toward finding a new practical and real way to correct presbyopia.

Acknowledgments

The authors thank all the subjects who participated in this study for their cooperation.

Supported by grants from Comité para el Desarrollo de la Investigación (CODI) and Estrategia de Sostenibilidad 2014-2015, Universidad de Antioquia-Colombia, and Grant FP44842-023-2015 from Fondo Nacional de Financiamiento para la Ciencia, la Tecnología y la Innovación Francisco José de Caldas (Colciencias-Colombia). Support was also provided by the Polish National Centre for Research and Development through the strategic scientific research and experimental development program "Model of intraocular lens providing extended depth of field" through Grant PBS/A9/23/2013. Production of the LSL elements was supported by LightSwords Grant FP7-SME-2012-315564 within the Seventh Framework Programme of the European Union. Additional support was provided by International Centre for Theoretical Physics ICTP Associateship Scheme (JFB).

Disclosure: **A. Mira-Agudelo**, None; **W. Torres-Sepúlveda**, None; **J.F. Barrera**, None; **R. Henao**, None; **N. Blocki**, None; **K. Petelczyc**, None; **A. Kolodziejczyk**, None

References

1. Atchison DA. Accommodation and presbyopia. *Ophthalmic Physiol Opt*. 1995;15:255–272.
2. Charman WN. The eye in focus: accommodation and presbyopia. *Clin Exp Optom*. 2008;91:207–225.
3. Jain S, Arora I, Azar DT. Success of monovision in presbyopes: review of the literature and potential applications to refractive surgery. *Surv Ophthalmol*. 1996;40:491–499.
4. Glasser A. Restoration of accommodation: surgical options for correction of presbyopia. *Clin Exp Optom*. 2010;91:279–295.
5. Back A, Grant T, Hine N. Comparative visual performance of three presbyopic contact lens corrections. *Optom Vis Sci*. 1992;69:474–480.
6. Seyeddain O, Riha W, Hohensinn M, Nix G, Dexl AK, Grabner G. Refractive surgical correction of presbyopia with the AcuFocus small aperture corneal inlay: two-year follow-up. *J Refract Surg*. 2010;26:707–715.
7. Vryghem JC, Heireman S. Visual performance after the implantation of a new trifocal intraocular lens. *Clin Ophthalmol*. 2013;7:1957–1965.
8. Mojzis P, Peña-García P, Liehneova I, Ziak P, Alió JL. Outcomes of a new diffractive trifocal intraocular lens. *J Cataract Refract Surg*. 2014;40:60–69.
9. García-Lazaro S, Ferrer-Blasco T, Radhakrishnan H, Cerviño A, Charman WN, Montés-Micó R. Visual function through 4 contact lens-based pinhole systems for presbyopia. *J Cataract Refract Surg*. 2012;38:858–865.
10. Simonov AN, Vdovin G, Rombach MC. Cubic optical elements for an accommodative intraocular lens. *Opt Express*. 2006;14:7757–7775.
11. Simonov AN, Vdovin G, Loktev M. Liquid-crystal intraocular adaptive lens with wireless control. *Opt Express*. 2007;15:7468–7478.
12. Li G, Valley P, Ayräs P, Mathine DL, Honkanen S, Peyghambarian N. High-efficiency switchable flat diffractive ophthalmic lens with three-layer electrode pattern and two-layer via structures. *Appl Phys Lett*. 2007;90:111105.
13. Zhang W, Aljasem K, Zappe H, Seifert A. Completely integrated, thermo-pneumatically tunable microlens. *Opt Express*. 2011;19:2347–2362.

14. Menapace R, Findl O, Kriechbaum K, Leydolt-Koeppl C. Accommodating intraocular lenses: a critical review of present and future concepts. *Graefes Arch Clin Exp Ophthalmol*. 2007;245:473–489.
15. Lesiewska-Junk H, Kałuzny J. Intraocular lens movement and accommodation in eyes of young patients. *J Cataract Refract Surg*. 2000;26:562–565.
16. Findl O, Kiss B, Petternel V, et al. Intraocular lens movement caused by ciliary muscle contraction. *J Cataract Refract Surg*. 2003;29:669–676.
17. Ares J, Flores R, Bara S, Jaroszewicz Z. Presbyopia compensation with a quartic axicon. *Optom Vis Sci*. 2005;82:1071–1078.
18. Dowski J, Cathey WT. Extended depth of field through wavefront coding. *Appl Opt*. 1995;34:1859–1866.
19. Romero LA, Millan MS, Jaroszewicz Z, Kołodziejczyk A. Double peacock eye optical element for extended focal depth imaging with ophthalmic applications. *J Biomed Opt*. 2012;17:046013.
20. Kołodziejczyk A, Bara S, Jaroszewicz Z, Sypek M. The light sword optical element – a new diffraction structure with extended depth of focus. *J Mod Opt*. 1990;37:1283–1286.
21. Ares García J, Bara S, Gómez-García M, Jaroszewicz Z, Kołodziejczyk A, Petelczyc K. Imaging with extended focal depth by means of the refractive light sword optical element. *Opt Express*. 2008;16:18371–18378.
22. Petelczyc K, Bara S, Ciro López A, et al. Imaging properties of the light sword optical element used as a contact lens in a presbyopic eye model. *Opt Express*. 2011;19:25602–25616.
23. Mikuła G, Jaroszewicz Z, Kołodziejczyk A, Petelczyc K, Sypek M. Imaging with extended focal depth by means of lenses with radial and angular modulation. *Opt Express*. 2007;15:9184–9193.
24. Kakarenko K, Ducin I, Grabowiecki K, et al. Assessment of imaging with extended depth-of-field by means of the light sword lens in terms of visual acuity scale. *Biomed Opt Express*. 2015;6:1738–1748.
25. Manzanera S, Prieto PM, Ayala DB, Lindacher JM, Artal P. Liquid crystal adaptive optics visual simulator: application to testing and design of ophthalmic optical element. *Opt Express*. 2007;15:16177–16188.
26. Petelczyc K, Ares García J, Bara S, et al. Strehl ratios characterizing optical elements designed for presbyopia compensation. *Opt Express*. 2011;19:8693–8699.
27. Petelczyc K, Bara S, Ciro López A, et al. Contrast transfer properties of the light sword optical element designed for presbyopia compensation. *J Eur Opt Soc Rapid Publ*. 2011;6:11053.
28. Liang J, Grimm B, Goelz S, Bille JF. Objective measurement of wave aberrations of the human eye with the use of a Hartmann-Shack wave-front sensor. *J Opt Soc Am A*. 1994;11:1949–1957.
29. Radhakrishnan H, Charman WN. Age-related changes in ocular aberrations with accommodation. *J Vis*. 2007;7(7):11.
30. World Medical Association. World Medical Association Declaration of Helsinki: ethical principles for medical research involving human subjects. *JAMA*. 2013;310:2191–2194.
31. Schwarz C, Manzanera S, Prieto PM, Fernández EJ, Artal P. Comparison of binocular through-focus visual acuity with monovision and a small aperture inlay. *Biomed Opt Express*. 2014;5:3355–3366.
32. Legras R, Benard Y, Rouger H. Through-focus visual performance measurements and predictions with multifocal contact lens. *Vision Res*. 2010;50:1185–1193.
33. Plainis S, Ntzilepis G, Atchison DA, Charman WN. Through-focus performance with multifocal contact lenses: effect of binocularity, pupil diameter and inherent ocular aberrations. *Ophthalmic Physiol Opt*. 2013;33:42–50.
34. Bach M. The Freiburg visual acuity test variability unchanged by post-hoc re-analysis. *Graefes Arch Clin Exp Ophthalmol*. 2007;245:965–971.
35. Goodman JW. *Introduction to Fourier Optics*. 2nd ed. New York: McGraw-Hill; 1996:126–165.
36. Kaufmann J, Schering A. Analysis of variance ANOVA. In: *Wiley StatsRef: Statistics Reference Online*. John Wiley & Sons, Inc.; 2014.
37. Atchison DA, Guo H, Fisher SW. Limits of spherical blur determined with an adaptive optics mirror. *Ophthalmol Physiol Opt*. 2009;29:300–311.
38. Cánovas C, Prieto PM, Manzanera S, Mira A, Artal P. Hybrid adaptive-optics visual simulator. *Opt Lett*. 2010;35:196–198.

Investigative Ophthalmology & Visual Science